



The Influence of Moisture on The Electronic Properties of Monomer, Dimer, Trimer and Emeraldine Base Sodium Carboxymethyl Cellulose



Rania Badry^{1*}, Sherif El-Khodary², Hanan Elhaes¹, Nadra Nada¹ and Medhat A. Ibrahim³

¹Physics Department, Faculty of Women for Arts, Science and Education, Ain Shams University, 11757 Cairo, Egypt.

²Building Physics and Environment Institute, Housing & Building National Research Center (HBRC), 12311 Dokki, Giza, Egypt.

³Spectroscopy Department, National Research Centre, 33 El-Bohouth St., 12622 Dokki, Giza, Egypt.

ACCORDING to previous studies on moisture effect, it is stated that moisture enhances the electronic properties of polymeric materials. A theoretical study based on density functional theory calculations at B3LYP/3-21G* is performed for investigating the effect of moisture on sodium carboxymethyl cellulose (Na-CMC) as monomer, dimer, trimer and emeraldine base. Results indicated that due to moisture, TDM is increased while HOMO/LUMO band gap energy is decreased for the four proposed structures for Na-CMC. All results indicated that there is a change occurring in the electronic properties as a result of moisture. Furthermore, as a result of increasing the degree of polymerization, the total dipole moment (TDM) of Na-CMC is increased and equals 7.7141, 28.0388, 24.0199 and 38.3464 Debye for monomer Na-CMC, dimer Na-CMC, trimer Na-CMC and emeraldine base Na-CMC respectively. However, the highest occupied and the lowest unoccupied energy gap (HOMO/LUMO band gap energy) decreased and equals 0.9040, 0.3448, 0.1241 and 0.9021 eV for the same sequence. Additionally, the results of ESP study of all model molecules are in good agreement with the results of TDM and HOMO/LUMO band gap energy.

Keywords: B3LYP/3-21G*; Na-CMC; TDM; HOMO/LUMO band gap energy and ESP.

Introduction

Cellulose derivative continued to be a topic of research interest according to its abundant, easy handling, biodegradation [1-3]. Carboxymethyl cellulose which is termed CMC, is one of famous examples of cellulose derivatives. Even it is considered as the most used cellulose derivatives in the industry. CMC, is a white-cream-colored powder, found in many industries such as in food, pharmaceutical, detergents and coatings. CMC shows an important application in the field of paper or textile improvement as fibers [4-7]. It could be

described as anionic linear polymer whereas the original H atom in cellulose hydroxyl group is replaced by carboxymethyl substituent ($-\text{CH}_2-\text{COO}^-$) [8]. CMC is strongly recommended as an additive in many commodity products according to its non-toxicity, high water solubility as well as the outstanding light and thermal stability [9]. As far as alkali is interacted with cellulose in aqueous NaOH with monochloro acetic acid or its sodium salt, CMCs with different degree of substitution (generally in the range 0.5–1.4 for commercial products) could be prepared [10].

*Corresponding author e-mail: raniabadry806@gmail.com

Received 28/2/2019; Accepted 28/5/2019

DOI: 10.21608/ejchem.2019.12805.1800

©2019 National Information and Documentation Center (NIDOC)

To produce cost effective CMC, there are several attempts to find out alternatives for cotton, such alternatives include lignocellulosic biomasses which is rich in cellulose [11-12]. Attempts are also continued in this trend to produce CMC from cellulose rich materials including aquatic plants and sugar as well as many agricultural residues [13-15]. Accordingly, understanding the structural and electronic properties of CMC is an important step toward further application of such important derivative. It is stated that, molecular modeling show potential to study natural polymers as well as many other emerging materials [16-19]. In this sense molecular modeling at B3LYP/3-21G* level is conducted to study the influence of moisture on the electronic properties of monomer, dimer, trimer and emeraldine base sodium carboxymethyl cellulose.

Computational Details

The effect of moisture on sodium carboxymethyl cellulose (Na-CMC) was studied using density functional theory (DFT) calculations at B3LYP/3-21G* [20-22]. Model molecules representing Na-CMC and hydrated Na-CMC are exposed to computations with GAUSSIAN09 [23] program at Spectroscopy Department, National Research Centre, Egypt. Total dipole moment (TDM) and HOMO/LUMO band gap energy are included in the performed computations using the same theoretical procedure. Additional calculations such as electrostatic potentials (ESP) are also performed for all models as contour action.

Results and Discussion

The geometry optimization of Na-CMC and Na-CMC-XH₂O where X=1, 2, 3, 4 and 5 molecules was performed to see how the presence of moisture affects the electronic properties of Na-CMC. Different geometries of Na-CMC are suggested where a large number of atoms are optimized to form Na-CMC with different degrees of polymerization, geometries and shapes. The influence of moisture on the sodium salt of carboxymethyl cellulose is studied at four different shapes which are monomer, dimer, trimer and emeraldine base. Model molecules which represent 1Na-CMC and moisturized 1Na-CMC, 2Na-CMC and moisturized 2Na-CMC, 3Na-CMC and moisturized 3Na-CMC and 4Na-CMC and moisturized 4Na-CMC are shown in Fig. 1, 2, 3 and 4 respectively.

Fig. 1(a), 2(a), 3(a) and 4(a) shows the

optimized structures of Na-CMC as a monomer (1Na-CMC), dimer (2Na-CMC), trimer (3Na-CMC) and emeraldine base (4Na-CMC) (which means one unit, two units, three units and four units of Na-CMC) respectively. It is necessary to study both TDM and HOMO/LUMO energies in order to study the influence of moisture on Na-CMC as they give direct information about the electronic properties and the behavior of electrons of the studied models due to moisture.

The correlation between reactivity and physical properties such as TDM and HOMO/LUMO band gap energy are reported earlier [23-24]. Reactivity increases directly with TDM and inversely with HOMO/LUMO band gap. Accordingly both values are calculated and reported as indicated in Table 1.

Table 1 presents the change in TDM (as Debye) and HOMO/LUMO band gap energies (as eV) for monomer Na-CMC and hydrated 1Na-CMC. The changes in both quantities are of most considerable effect on the electronic properties. As for 1Na-CMC, the values of TDM increases to approximately to twice due to increasing moisture level, but for energies of band gaps of 1Na-CMC decreases strongly. As a result of optimization, TDM of 1Na-CMC increased with moisture from 7.7141, 11.4010, 15.6974, 17.3795, 18.3347 and 20.4391 Debye for 1Na-CMC, 1Na-CMC-1H₂O, 1Na-CMC-2H₂O, 1Na-CMC-3H₂O, 1Na-CMC-4H₂O and 1Na-CMC-5H₂O respectively. However, HOMO/LUMO band gap energy of 1Na-CMC changed as shown in Fig. 5 and decreased from 0.9040 eV for 1Na-CMC to 0.6645, 0.2275, 0.3042, 0.3440 and 0.2068 eV for, 1Na-CMC-1H₂O, 1Na-CMC-2H₂O, 1Na-CMC-3H₂O, 1Na-CMC-4H₂O and 1Na-CMC-5H₂O respectively.

For dimer Na-CMC that is for dimer Na-CMC, the changes occurred in TDM as well as HOMO/LUMO band gaps are presented in Table 2. TDM value of 2Na-CMC is found to be larger than that for 1Na-CMC and it is still increase with increasing the amount of moisture. Whereas a consequence of computations, TDM changed from 28.0388 Debye to 27.2369, 26.1905, 27.1086, 30.1295 and 34.2435 Debye for 2Na-CMC-1H₂O, 2Na-CMC-2H₂O, 2Na-CMC-3H₂O, 2Na-CMC-4H₂O and 2Na-CMC-5 H₂O respectively. On the other hand, HOMO/LUMO band gap energies also are influenced and this is clear from Fig. 6. HOMO/LUMO band gap energy of 2Na-CMC changed

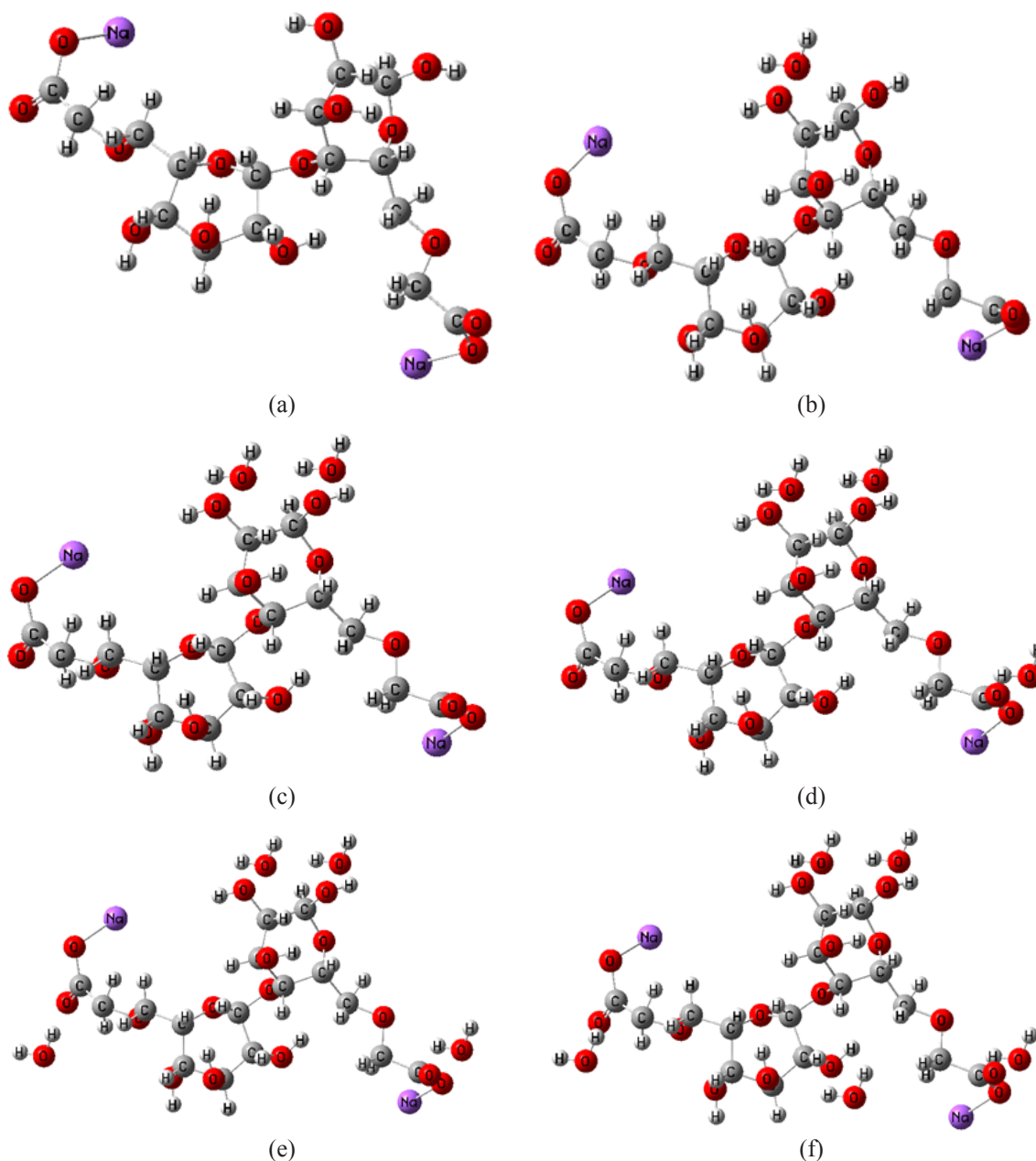


Fig. 1. B3LYP/3-21G* optimized model molecules for: a) 1Na-CMC; b) 1Na-CMC-1H₂O; c) 1Na-CMC-2H₂O; d) 1Na-CMC-3H₂O; e) 1Na-CMC-4H₂O; and f) 1Na-CMC-5H₂O.

from 0.3448 eV to 0.6950, 0.2917, 0.2857, 0.2610 and 0.4762 eV for 2Na-CMC-1 H₂O, 2Na-CMC-2 H₂O, 2Na-CMC-3H₂O, 2Na-CMC-4 H₂O and 2Na-CMC-5 H₂O respectively.

Similarly for trimer Na-CMC, TDM increases with increasing number of water molecules where it increases from 24.0199 Debye to 24.2442, 33.1871, 33.1868, 33.6315 and 34.2315 Debye which corresponding to 3Na-CMC-1H₂O, 3Na-

CMC-2H₂O, 3Na-CMC-3H₂O, 3Na-CMC-4H₂O and 3Na-CMC-5H₂O respectively. Meanwhile, the band gap energy of 3Na-CMC changed as shown in Fig. 7 from 0.1241 eV to 0.1244, 0.1195, 0.1195, 0.1195 and 0.1197 eV for 3Na-CMC-1H₂O, 3Na-CMC-2H₂O, 3Na-CMC-3H₂O, 3Na-CMC-4H₂O and 3Na-CMC-5H₂O respectively. It is evidence that the increase in TDM and the decrease in HOMO/LUMO band gap energy values for trimer Na-CMC is slightly small and

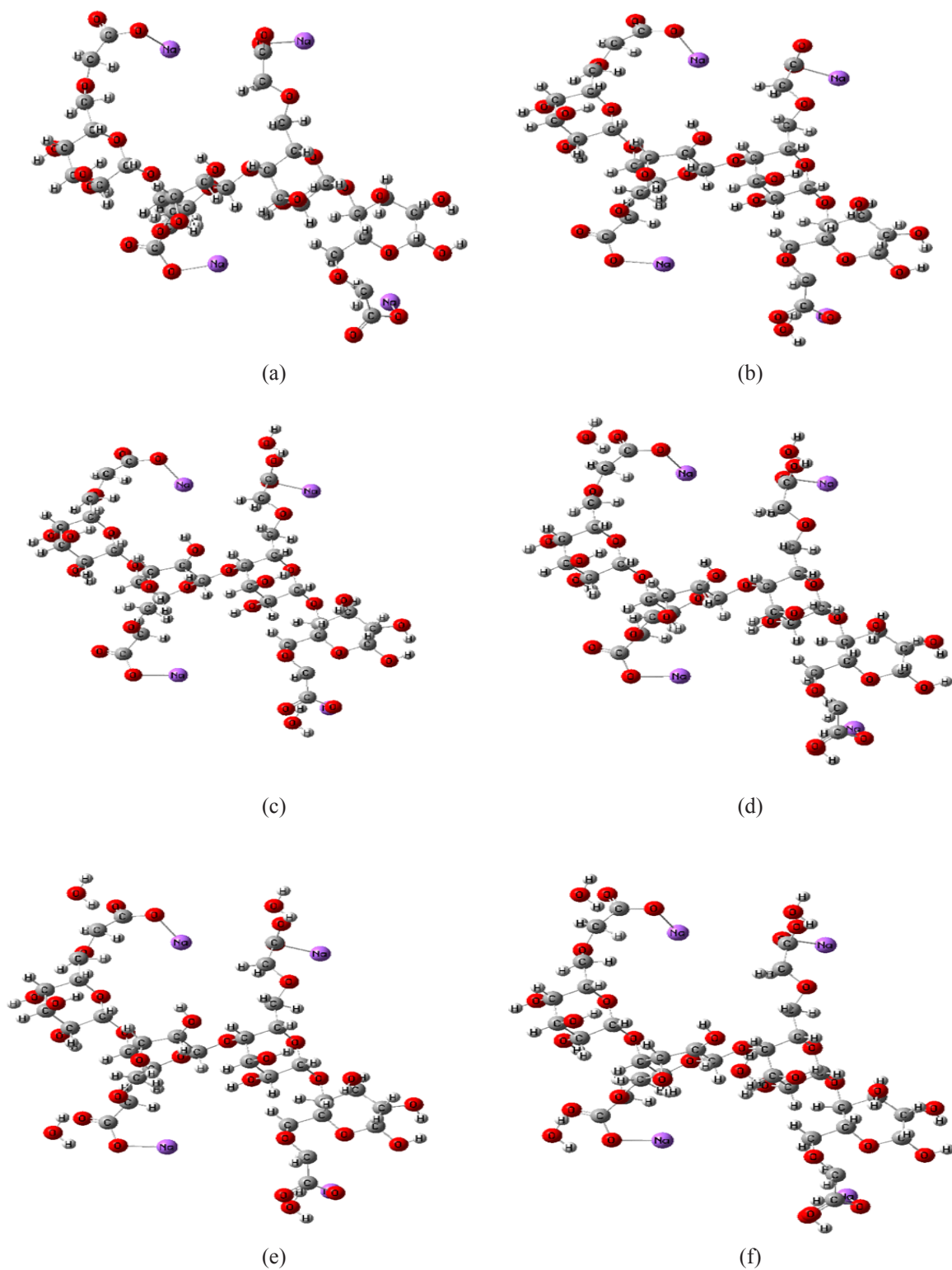


Fig. 2. B3LYP/3-21G* optimized model molecules for: a) 2Na-CMC; b) 2Na-CMC-1H₂O; c) 2Na-CMC-2H₂O; d) 2Na-CMC-3H₂O; e) 2Na-CMC-4H₂O; and f) 2Na-CMC-5H₂O.

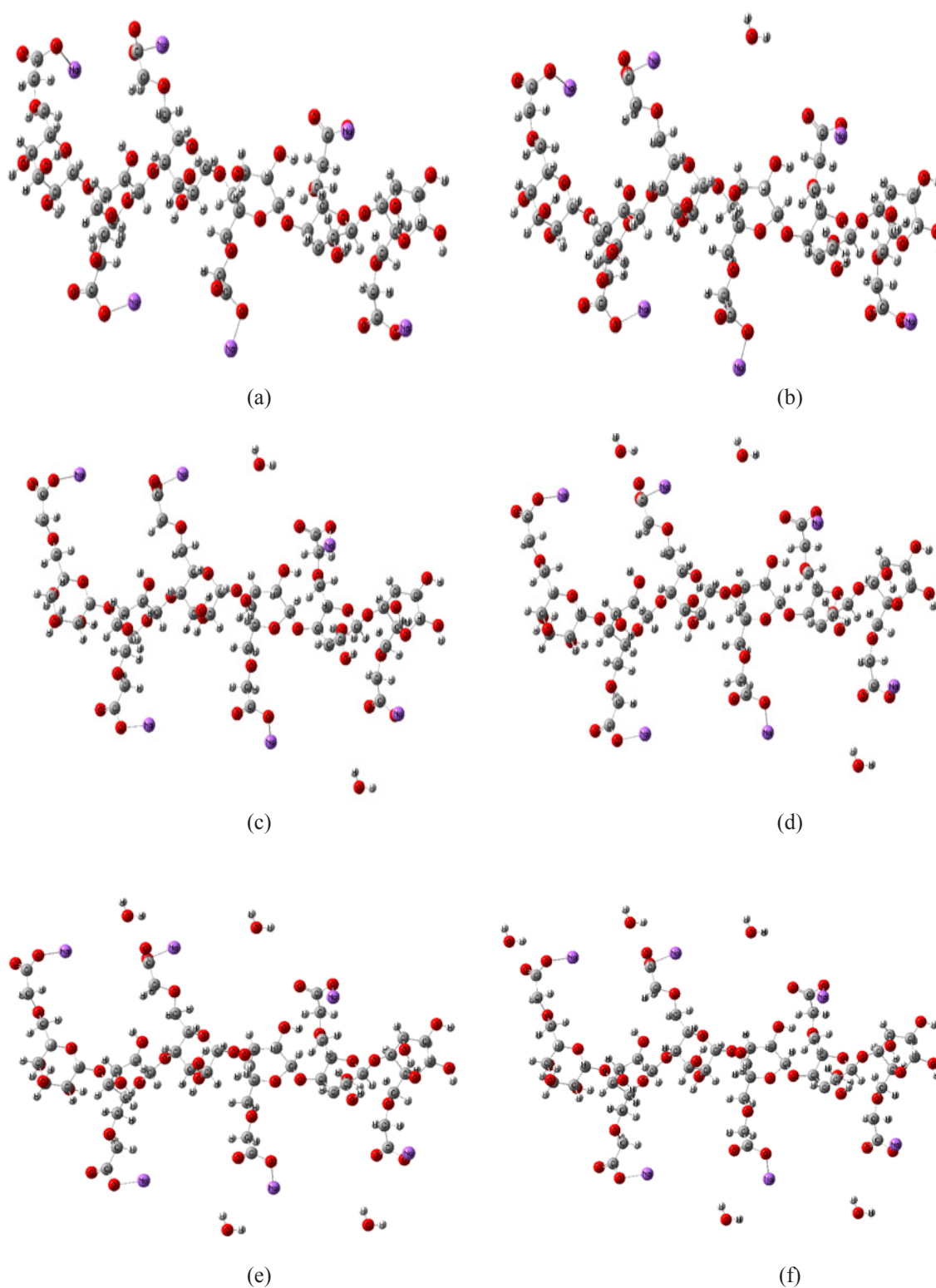


Fig. 3. B3LYP/3-21G* optimized model molecules for: a) 3Na-CMC; b) 3Na-CMC-1H₂O; c) 3Na-CMC-2H₂O; d) 3Na-CMC-3H₂O; e) 3Na-CMC-4H₂O; and f) 3Na-CMC-5H₂O.

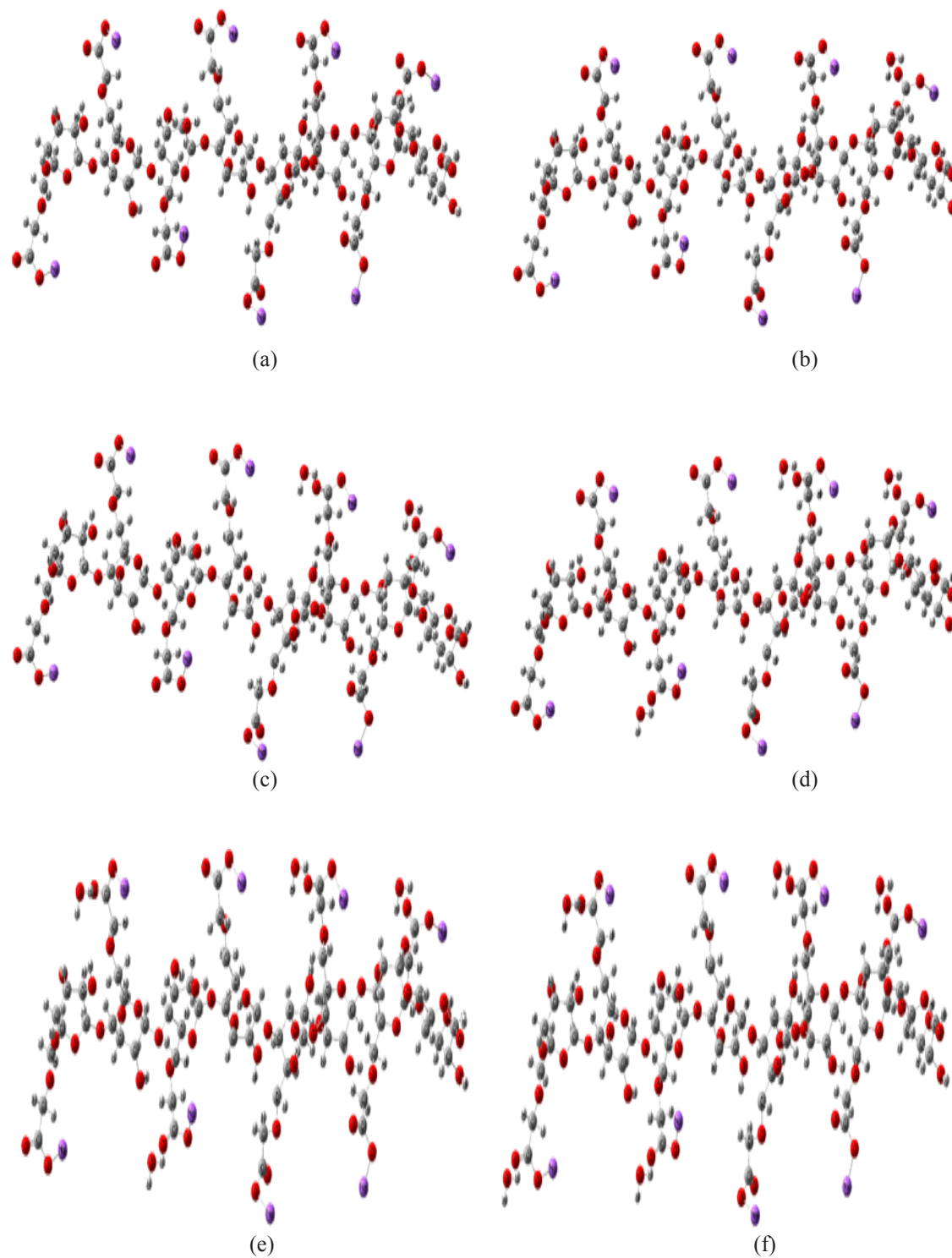


Fig. 4. B3LYP/3-21G* optimized model molecules for: a) 4Na-CMC; b) 4Na-CMC-1H₂O; c) 4Na-CMC- 2H₂O; d) 4Na-CMC-3H₂O; e) 4Na-CMC-4H₂O; and f) 4Na-CMC-5H₂O.

TABLE 1. B3LYP/3-21G* calculated total dipole moment (TDM) as Debye; HOMO-LUMO band gap energy (ΔE) as eV for 1Na-CMC and 1Na-CMC-XH₂O where X=1, 2, 3, 4 and 5.

Structure	TDM	ΔE
1Na-CMC	7.7141	0.9040
1Na-CMC-1 H ₂ O	11.4010	0.6645
1Na-CMC-2 H ₂ O	15.6974	0.2275
1Na-CMC-3 H ₂ O	17.3795	0.3042
1Na-CMC-4 H ₂ O	18.3347	0.3440
1Na-CMC-5 H ₂ O	20.4391	0.2068

TABLE 2. B3LYP/3-21G* calculated total dipole moment (TDM) as Debye; HOMO-LUMO band gap energy (ΔE) as eV for 2Na-CMC and 2Na-CMC-XH₂O where X=1, 2, 3, 4 and 5.

Structure	TDM	ΔE
2Na-CMC	28.0388	0.3448
2Na-CMC-1 H ₂ O	27.2369	0.6950
2Na-CMC-2 H ₂ O	26.1905	0.2917
2Na-CMC-3 H ₂ O	27.1086	0.2857
2Na-CMC-4 H ₂ O	30.1295	0.2610
2Na-CMC-5 H ₂ O	34.2435	0.4762

they are considered approximately constant for more than single water molecule.

Finally, forearmidine base Na-CMC, both quantities TDM and HOMO/LUMO band gaps respectively are affected by moisture and their values changed as listed in Table 4 from 38.3464 Debye and 0.9021 eV to 49.1728, 50.6196, 50.1925, 31.2450 and 51.4272 Debye and to 0.1551, 0.1554, 0.1535, 0.4123 and 0.1535 eV corresponding to 4Na-CMC, 4Na-CMC-1H₂O, 4Na-CMC-2H₂O, 4Na-CMC-3H₂O, 4Na-CMC-4H₂O and 4Na-CMC-5H₂O respectively. Also it is evidence that, both TDM and HOMO/LUMO band gap energies are exposed to an enhancement in their values with increasing the number of Na-CMC units. Fig. 8 indicates the decrease in HOMO/LUMO bands due to moisturization. As TDM of monomer Na-CMC which is 7.7141 Debye increases to 28.0388, 24.0199 and 38.3464 Debye with increasing the degree of polymerization to 2Na-CMC, 3Na-CMC and 4Na-CMC respectively. However, HOMO/LUMO band gap energy of 1Na-CMC decreased from 0.9040 eV to 0.3448, 0.1241 and 0.9021

ev for 2Na-CMC, 3Na-CMC and 4Na-CMC respectively.

Also it is clear that, the lowest band gap energy obtained for monomer Na-CMC and emeraldine base Na-CMC is obtained when Na-CMC in its form is interacted with five water molecules but for dimer and trimer Na-CMC the lowest band gap energy obtained is obtained when the interacted was done with four water molecules.

Another correlation between reactivity and physical properties is indicated in terms the molecular electrostatic potential as stated earlier [25-27]. The ESP is mapped in this work as an indicator for reactivity of the studied structures.

Besides all these results, also electrostatic potentials (ESPs) are calculated for all models under investigation using the same laws of quantum mechanics. The importance of ESP study lies in its ability to give more explanation about the distribution of the charges of molecules which illustrates how the studied structures can interact with moisture. Fig. 9,10, 11 and 12 shows the calculated ESPs as contour for the

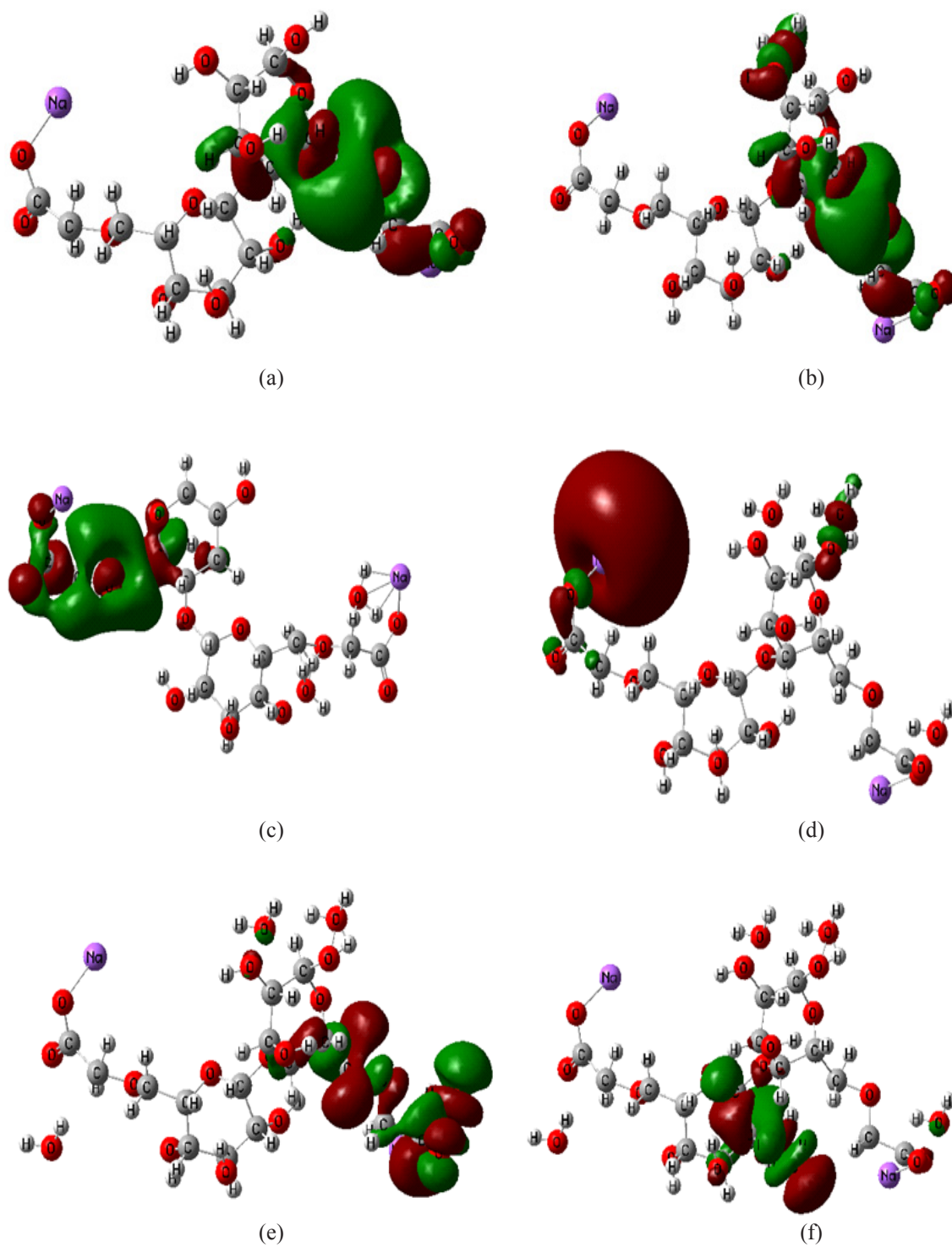


Fig. 5. B3LYP/3-21G* optimized HOMO/LUMO band gap energy for: a) 1Na-CMC; b) 1Na-CMC-1H₂O; c) 1Na-CMC-2H₂O; d) 1Na-CMC-3H₂O; e) 1Na-CMC-4H₂O; and f) 1Na-CMC-5H₂O.

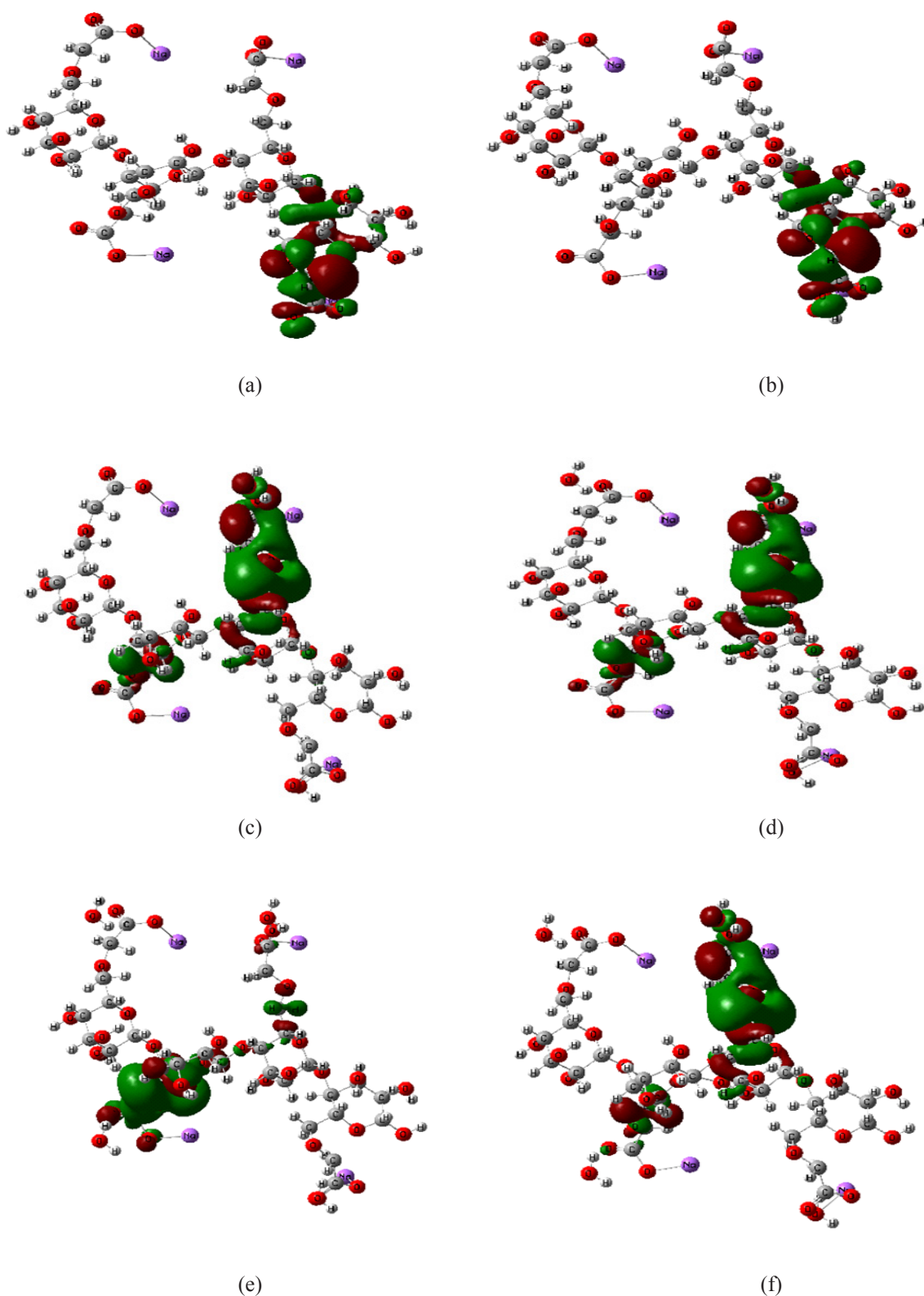


Fig. 6. B3LYP/3-21G* optimized HOMO/LUMO band gap energy for: a) 2Na-CMC; b) 2Na-CMC-1H₂O; c) 2Na-CMC-2H₂O; d) 2Na-CMC- 3H₂O; e) 2Na-CMC- 4H₂O; and f) 2Na-CMC-5H₂O.

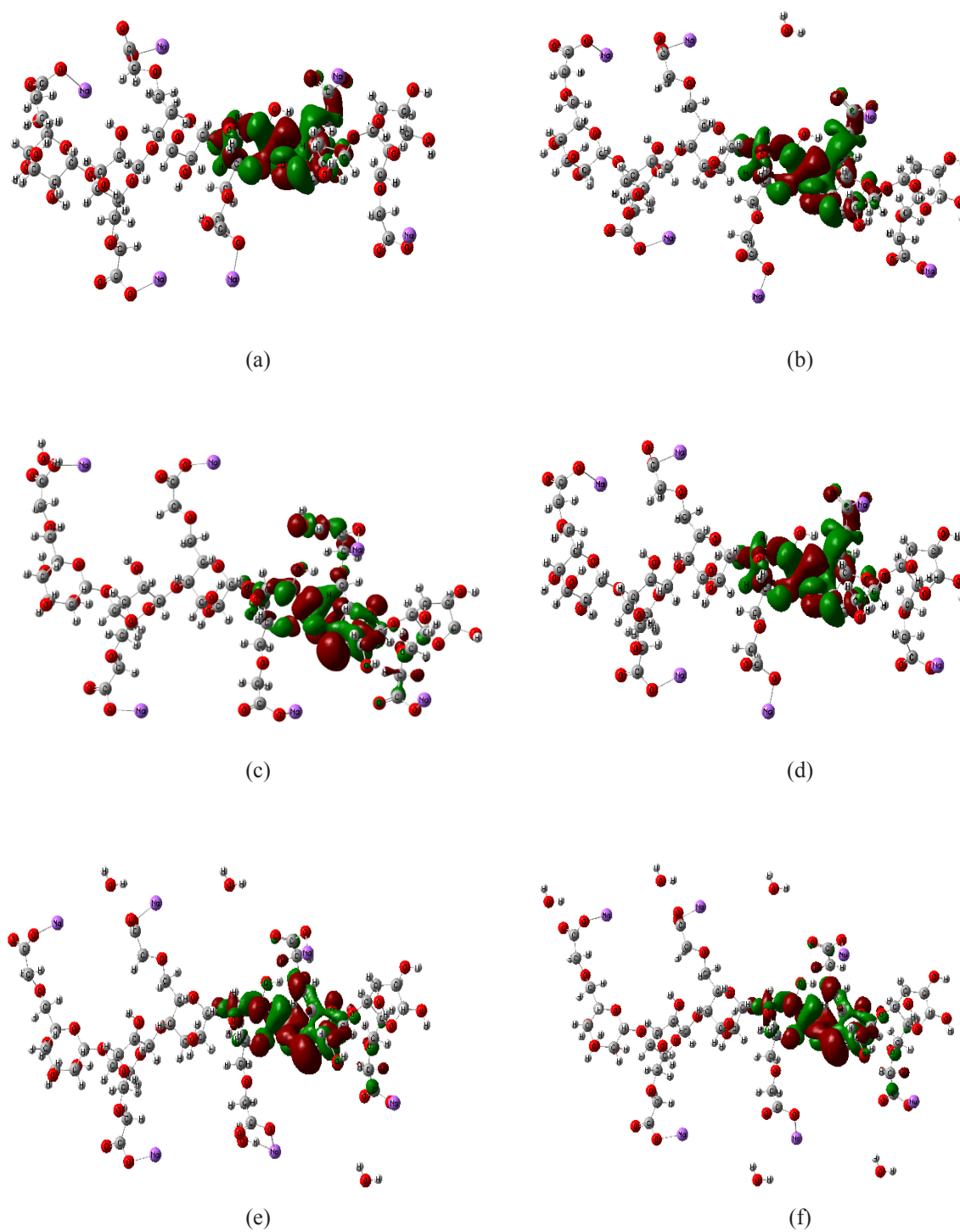


Fig. 7. B3LYP/3-21G* optimized HOMO/LUMO band gap energy for: a) 3Na-CMC; b) 3Na-CMC-1H₂O; c) 3Na-CMC-2H₂O; d) 3Na-CMC-3H₂O; e) 3Na-CMC-4H₂O; and f) 3Na-CMC-5H₂O.

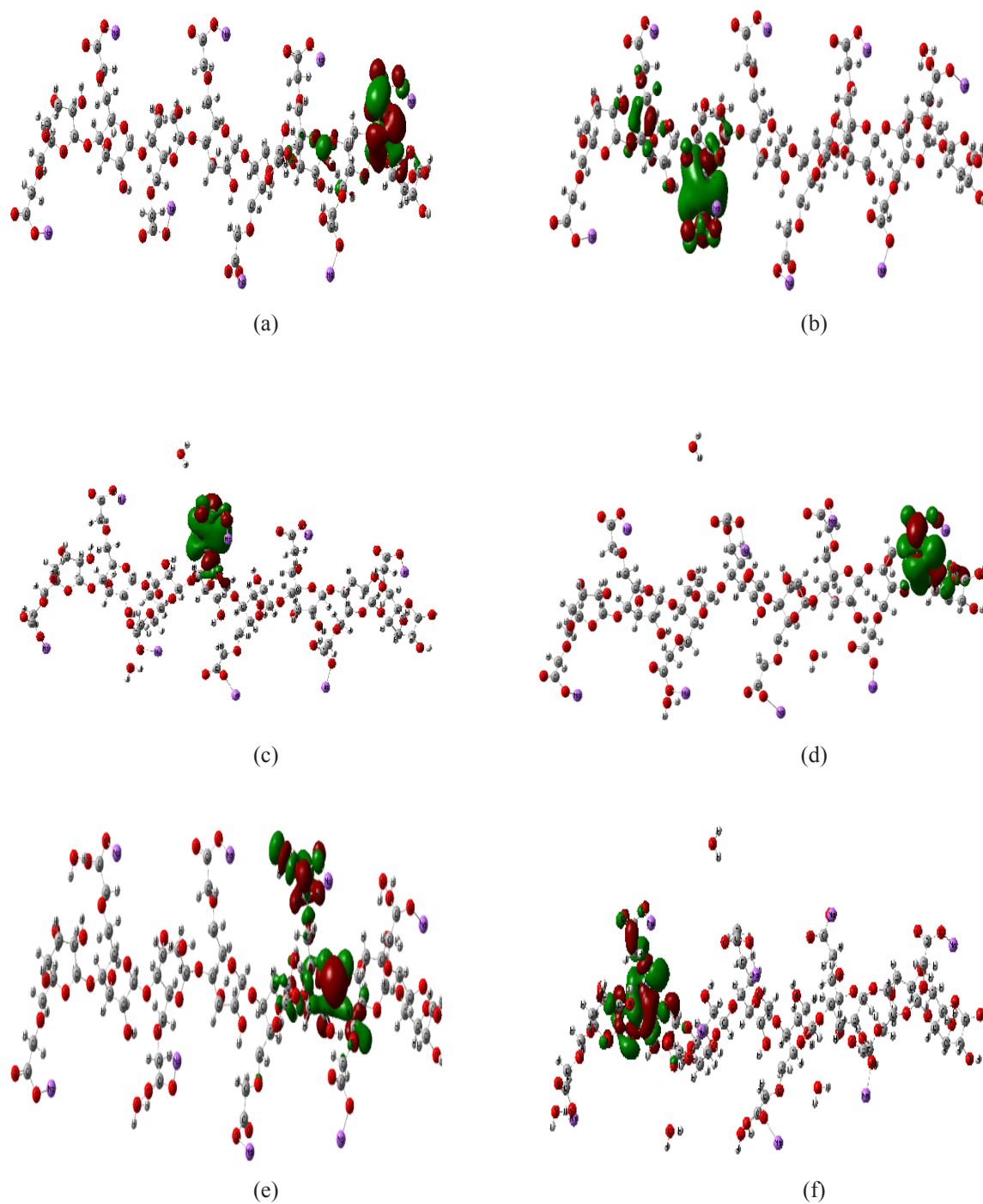


Fig. 8. B3LYP/3-21G* optimized HOMO/LUMO band gap energy for: a) 4Na-CMC; b) 4Na-CMC-1H₂O; c) 4Na-CMC-2H₂O; d) 4Na-CMC-3H₂O; e) 4Na-CMC-4H₂O; and f) 4Na-CMC-5H₂O.

TABLE 3. B3LYP/3-21G* calculated total dipole moment (TDM) as Debye; HOMO-LUMO band gap energy (ΔE) as eV for 3Na-CMC and 3Na-CMC-XH₂O where X=1, 2, 3, 4 and 5.

Structure	TDM	ΔE
3 Na-CMC	24.0199	0.1241
3 Na-CMC-1H ₂ O	24.2442	0.1244
3 Na-CMC-2H ₂ O	33.1871	0.1195
3 Na-CMC-3H ₂ O	33.1868	0.1195
3 Na-CMC-4H ₂ O	33.6315	0.1195
3 Na-CMC-5H ₂ O	34.2315	0.1197

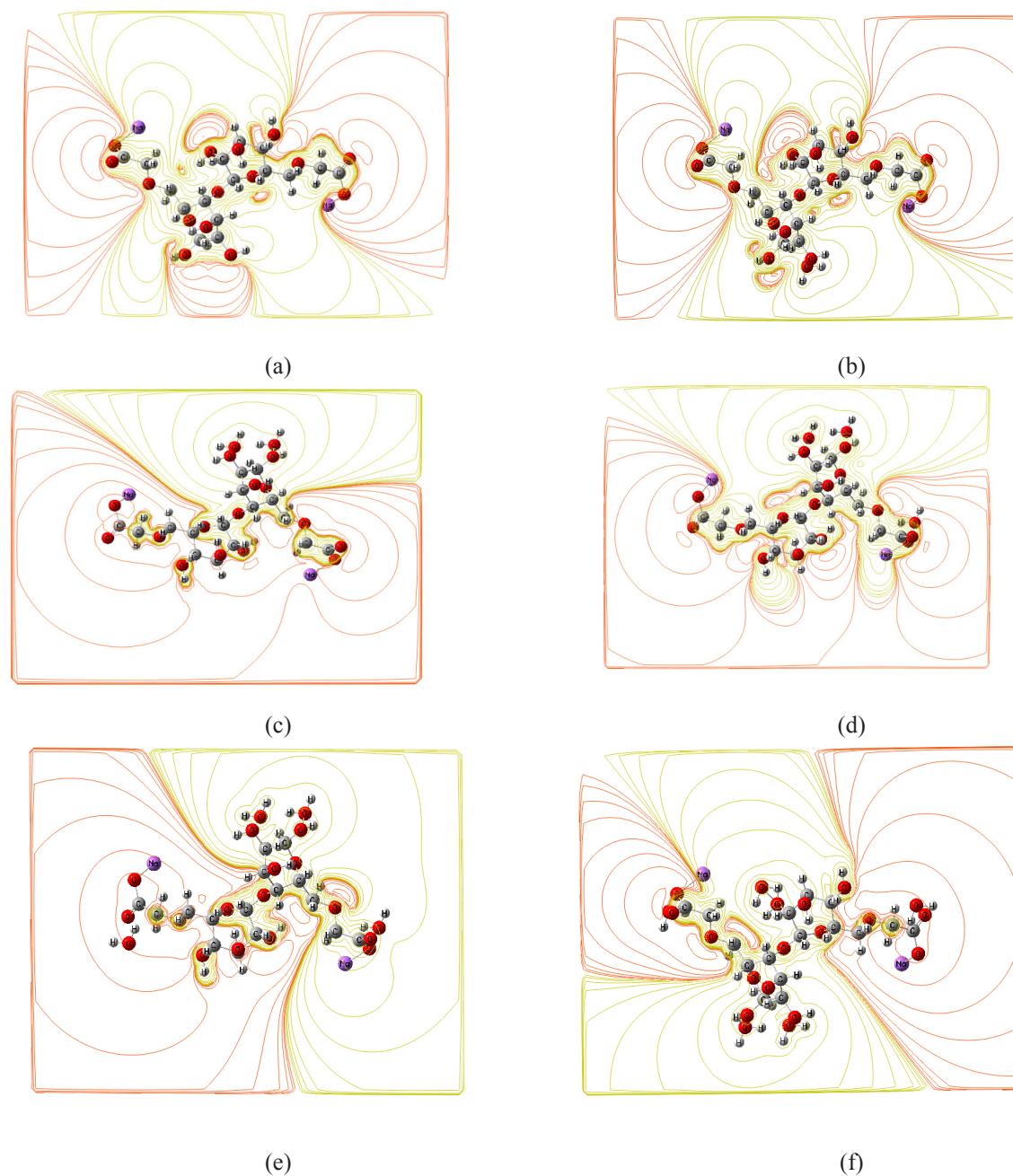


Fig. 9. B3LYP/3-21G* calculated ESP as contour for: a) 1Na-CMC; b) 1Na-CMC-1H₂O; c) 1Na-CMC-2H₂O; d) 1Na-CMC-3H₂O; e) 1Na-CMC-4H₂O; and f) 1Na-CMC-5H₂O.

TABLE 4. B3LYP/3-21G* calculated total dipole moment (TDM) as Debye; HOMO-LUMO band gap energy (ΔE) as eV for 4Na-CMC and 4Na-CMC-XH₂O where X=1, 2, 3, 4 and 5.

Structure	TDM	ΔE
4 Na-CMC	38.3464	0.9021
4 Na-CMC-1H ₂ O	49.1728	0.1551
4 Na-CMC-2H ₂ O	50.6196	0.1554
4 Na-CMC-3H ₂ O	50.1925	0.1535
4 Na-CMC-4H ₂ O	31.2450	0.4123
4 Na-CMC-5H ₂ O	51.4272	0.1535

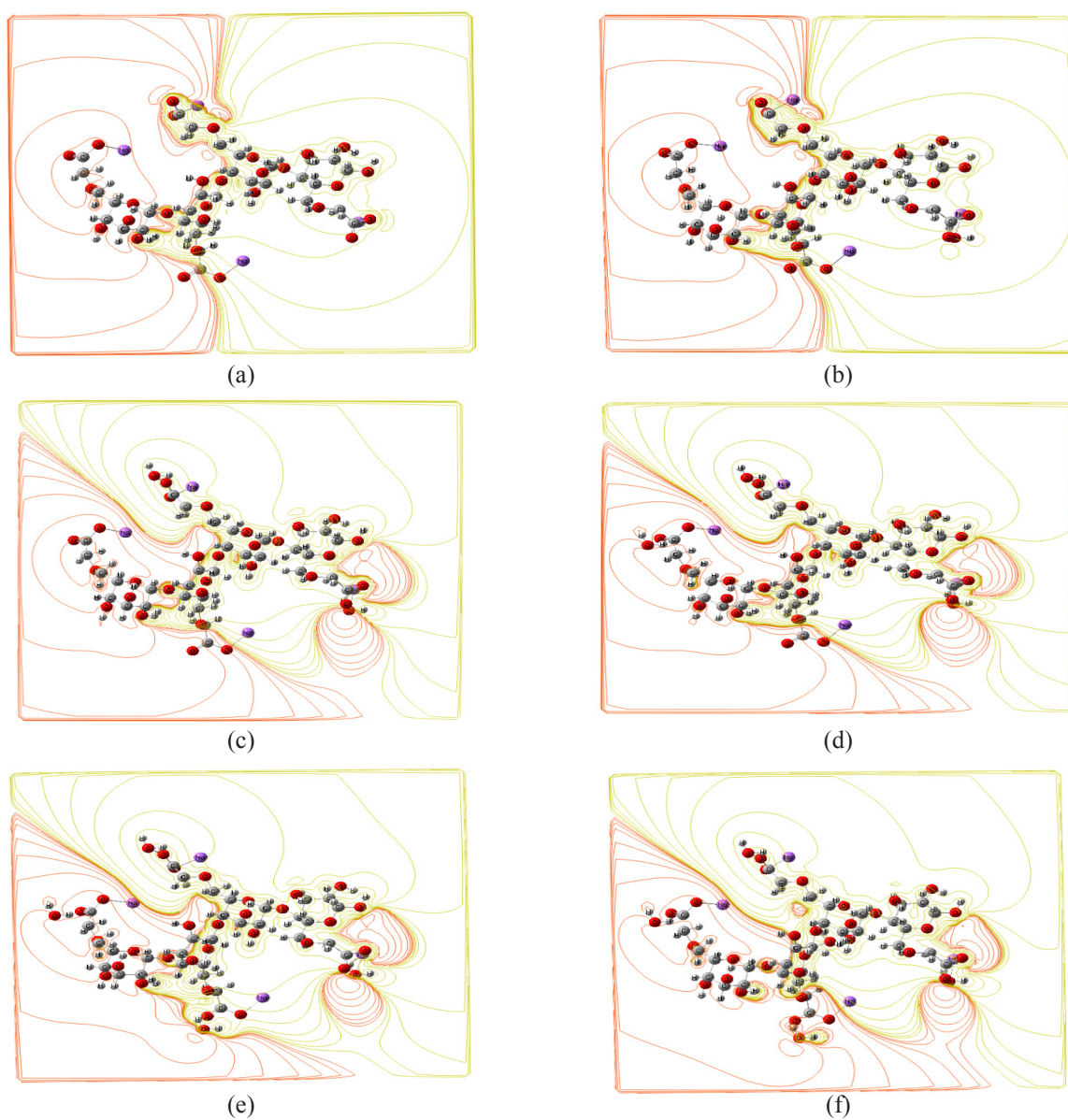


Fig. 10. B3LYP/3-21G* calculated ESP as contour for: a) 2Na-CMC; b) 2Na-CMC-1H₂O; c) 2Na-CMC-2H₂O; d) 2Na-CMC-3H₂O; e) 2Na-CMC-4H₂O; and f) 2Na-CMC-5H₂O.

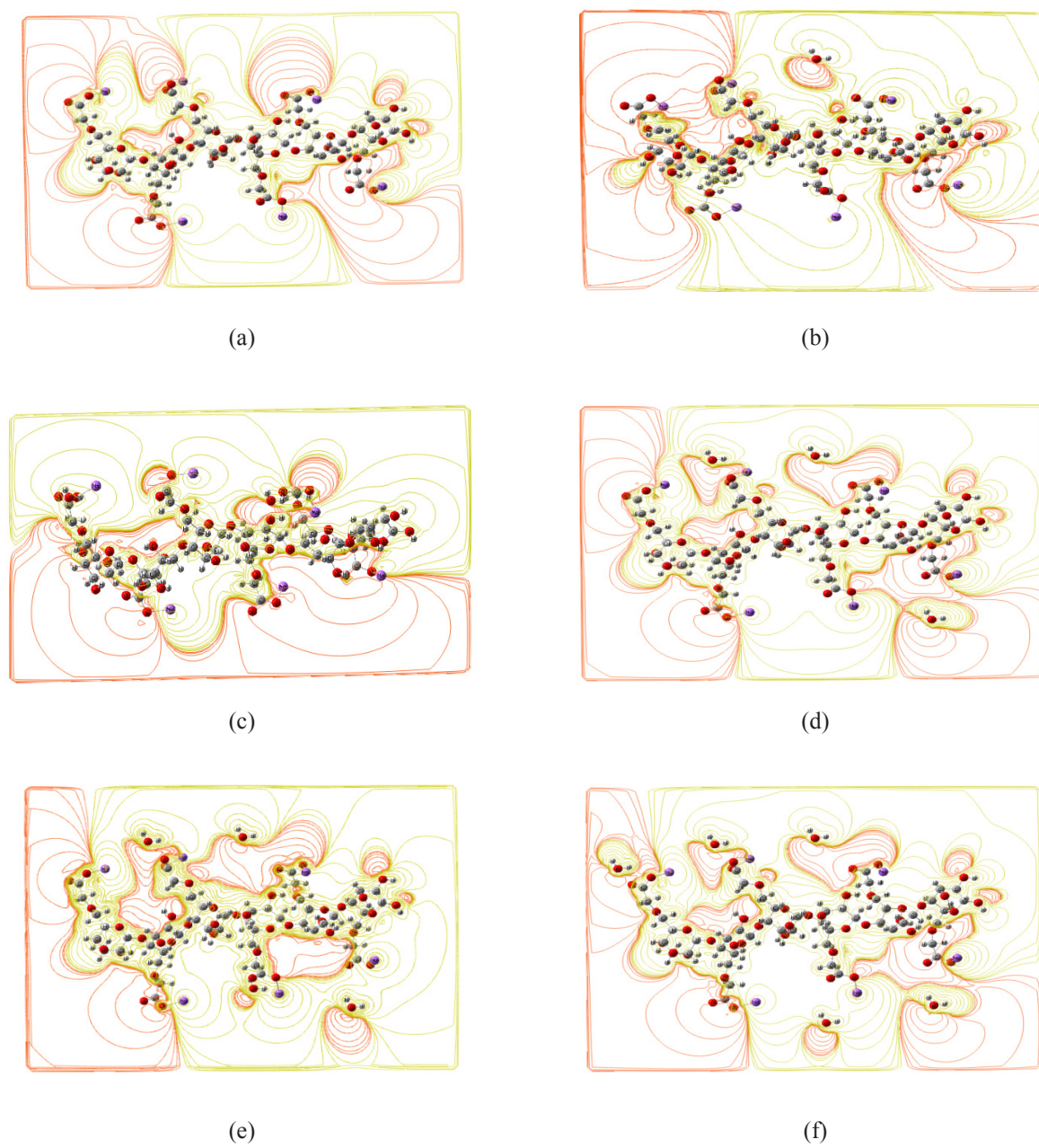


Fig. 11. B3LYP/3-21G* calculated ESP as contour for: a) 3Na-CMC; b) 3Na-CMC-1H₂O; c) 3Na-CMC- 2H₂O; d) 3Na-CMC-3H₂O; e) 3Na-CMC-4H₂O; and f) 3Na-CMC-5H₂O.

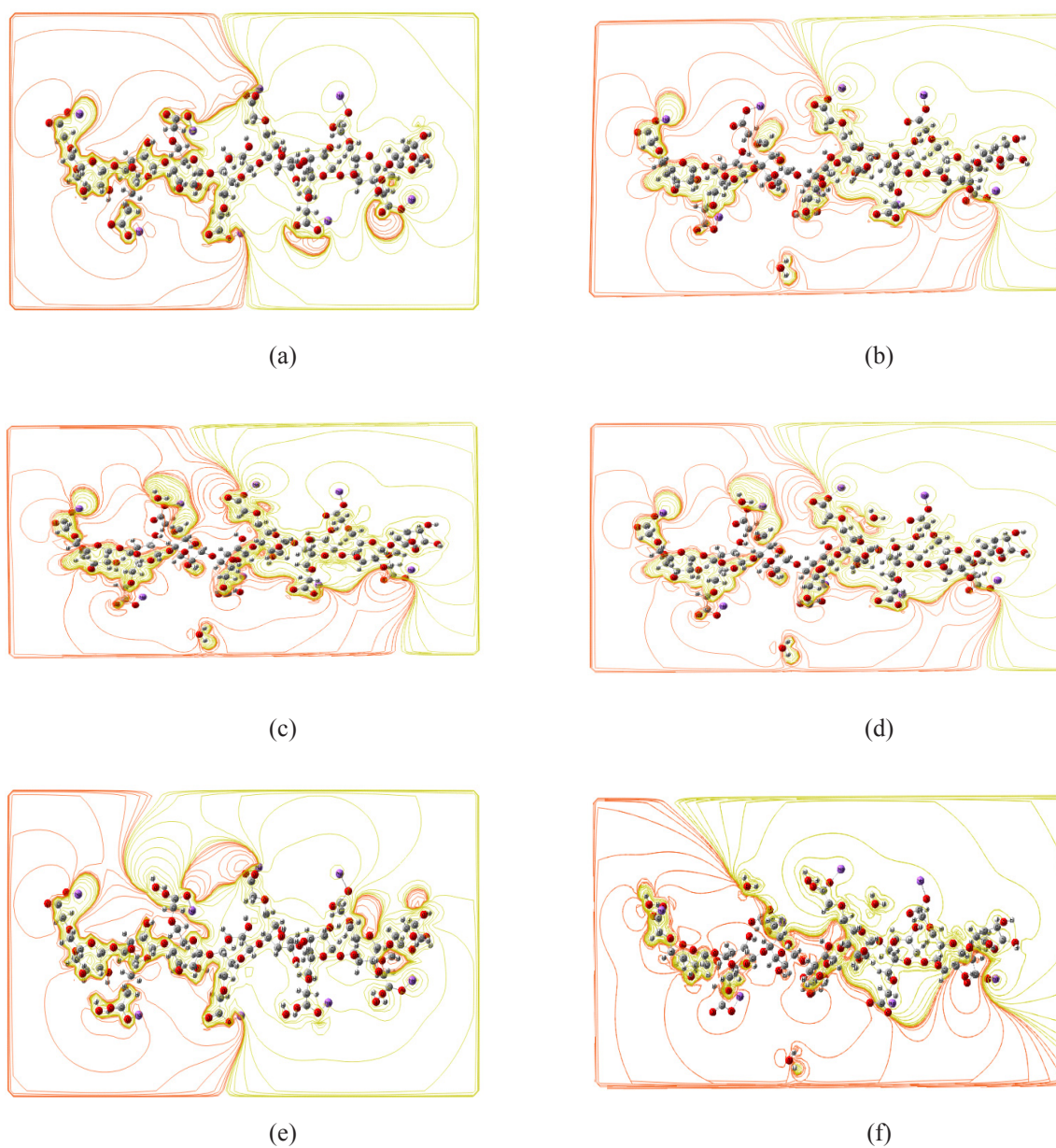


Fig. 12. B3LYP/3-21G* calculated ESP as contour for: a) 4Na-CMC; b) 4Na-CMC-1H₂O; c) 4Na-CMC-2H₂O; d) 4Na-CMC-3H₂O; e) 4Na-CMC- 4H₂O; and f) 4Na-CMC-5H₂O.

four different geometries of Na-CMC and that which are subjected to moisture. Where Fig. 9b shows the calculated electrostatic potentials at B3LYP/3-21G* basis set for a)1Na-CMC, b)1Na-CMC-1H₂O, b)1Na-CMC-2H₂O, b)1Na-CMC-3H₂O, b)1Na-CMC-4H₂O and b)1Na-CMC-5H₂O as contour view. Also Fig. 10 presents ESPs for a)2Na-CMC, b)2Na-CMC-1H₂O, b)2Na-CMC-2H₂O, b)2Na-CMC-3H₂O, b)2Na-CMC-4H₂O and b)2Na-CMC-5H₂O. Similarly Fig. 11 and 12 presents the B3LYP/3-21G* calculated ESP for a)3Na-CMC, b)3Na-CMC-1H₂O, b)3Na-CMC-2H₂O, b)3Na-CMC-3H₂O, b)3Na-CMC-4H₂O, b)3Na-CMC-5H₂O and for a)4Na-CMC, b)4Na-CMC-1H₂O, b)4Na-CMC-2H₂O, b)4Na-CMC-3H₂O, b)4Na-CMC-4H₂O and b)4Na-CMC-5H₂O respectively. ESPs can be expressed by following mapped colors. The colors express the electro-negativity level which decreases on going from red to orange, yellow, green and blue. As shown in the mentioned Fig. that, as a result of moisture content, the red color increased around 1Na-CMC, 2Na-CMC, 3Na-CMC and 4Na-CMC due to moisture for all of the investigated individual structures.

Also the electro-negativity of Na-CMC increases with increasing the degree of polymerization from 1Na-CMC to 2Na-CMC, 3Na-CMC and 4Na-CMC. Finally, all these enhancements in the electro-negativity indicates that their activity increases.

Conclusion

To depict the influence of moisture on the four different shapes of Na-CMC, both the total dipole moment (TDM) and HOMO/LUMO band gap energy are calculated. As a result of moisture, in all cases, the TDM of Na-CMC was increased while HOMO/LUMO band gap energy decreased. The highest value of TDM for monomer Na-CMC is 20.4391 Debye and the lowest value of HOMO/LUMO band gap energy is 0.2068 eV which are for 1Na-CMC-5H₂O. However, for dimer Na-CMC the highest value of TDM is 30.1295 Debye and the lowest value of HOMO/LUMO band gap energy is 0.2610 eV which are for 2Na-CMC-4H₂O but for trimer Na-CMC are 33.6315 Debye and 0.1195 eV respectively for 3Na-CMC-4H₂O. Finally, for emeraldine base the highest value of TDM is 51.4272 Debye and the lowest value of HOMO/LUMO band gap energy is 0.1535 eV which are for 4Na-CMC-5H₂O. Also the values of TDM increases with increasing the degree of polymerization whereas HOMO/LUMO band gap

energy decreases. All these effects indicate that the reactivity of the studied structures increases and hence the electronic properties are enhanced greatly. Furthermore, ESP results indicated that the electronic properties are enhanced due to moisture as the electron cloud increases.

References

1. Wang Y., Groszewicz P.B., Rosenfeldt S., Schmidt H., Volkert C.A., Vana P., Gutmann T., Buntkowsky G., Zhang K.; Thermoreversible self-assembly of perfluorinated core-coronas cellulose-nanoparticles in dry state, *Adv. Mater.*, **29**(43), 1702473 (2017).
2. Rong L., Zeng M., Liu H., Wang B., Mao Z., Xu H., Zhang L., Zhong Y., Yuan J., Sui X.; Biginelli Reaction on Cellulose Acetoacetate: A New Approach for Versatile Cellulose Derivatives, *Carbohydr. Polym.*, **209**, 223-229 (2019).
3. Grönroos P., Salminen K., Paltakari J., Zhang Q., Wei N., Kauppinen E., Kulmala S.; Hot electron-induced electrochemiluminescence at cellulose derivatives-based composite electrodes, *J. Electroanal. Chem.*, **833**, 349-356 (2019).
4. Fijan R., Basile M., Šostar-Turk S., Žagar E., Žigon M., Lapasin R.; A study of rheological and molecular weight properties of recycled polysaccharides used as thickeners in textile printing, *Carbohydr. Polym.*, **76**(1), 8-16 (2009).
5. Toğrul H., Arslan N.; Production of carboxymethyl cellulose from sugar beet pulp cellulose and rheological behaviour of carboxymethyl cellulose, *Carbohydr. Polym.*, **54**(1), 73-82 (2003).
6. Xue J., Ngadi M.; Effects of methylcellulose, xanthan gum and carboxymethylcellulose on thermal properties of batter systems formulated with different flour combinations, *Food hydrocolloid*, **23**(2), 286-295 (2009).
7. Heinze T.; New ionic polymers by cellulose functionalization, *Macromol. Chem. Phys.*, **199**(11), 2341-2364 (1998).
8. Keller J.D., Sodium carboxymethylcellulose (CMC), in: "Food Hydrocolloids", Glicksman M. ed., Vol. 3, CRC Press, Boca Raton, 45-104 (1986).
9. Wang X., Zhai Y., Zhan W.; Determination of the degree of substitution of carboxymethyl cellulose sodium, *Journal of Food Safety and Quality*, **6**(8), 3145-3146 (2015).
10. Adinugraha M.P., Marseno D.W.; Synthesis and

- characterization of sodium carboxymethylcellulose from cavendish banana pseudo stem (*Musa cavendishii* LAMBERT), *Carbohyd. Polym.*, **62**(2), 164-169 (2005).
11. Toğrul H., Arslan N.; Production of carboxymethyl cellulose from sugar beet pulp cellulose and rheological behaviour of carboxymethyl cellulose, *Carbohyd. Polym.*, **54**(1), 73-82 (2003).
 12. Han C., Wang C., Jin T., Chu F.; Preparation of carboxymethyl cellulose by using bio-butanol by-product as raw material, *Biomass Chemical Engineering*, **6**(4), 40-45 (2010).
 13. Candido R.G., Gonçalves A.R.; Synthesis of cellulose acetate and carboxymethylcellulose from sugarcane straw, *Carbohyd. Polym.*, **152**, 679-686 (2016).
 14. Tijssen C.J., Kolk H.J., Stamhuis E.J., Beenackers A.A.C.M.; An experimental study on the carboxymethylation of granular potato starch in non-aqueous media, *Carbohyd. Polym.*, **45**(3), 219-226 (2001).
 15. Abdelsalam H., Saroka V.A., Ali M., Teleb N.H., Elhaes H., Ibrahim M.A.; Stability and electronic properties of edge functionalized silicene quantum dots: A first principles study, *Physica E*, **108**, 339-346 (2019).
 16. Galal A.M., Atta D., Abouelsayed A., Ibrahim M.A., Hanna A.G.; Configuration and molecular structure of 5-chloro-N-(4-sulfamoylbenzyl) salicylamide derivatives, *Spectrochim. Acta A*, **214**, 476-486 (2019).
 17. Abdelsalam H., Teleb N.H., Yahia I.S., Zahran H.Y., Elhaes H., Ibrahim M.A.; First principles study of the adsorption of hydrated heavy metals on graphene quantum dots, *J. Phys. Chem. Solids*, **130**, 32-40 (2019).
 18. Galal A.M.F., Shalaby E.M., Abouelsayed A., Ibrahim M.A., Al-Ashkar E., Hanna A.G.; Structure and absolute configuration of some 5-chloro-2-methoxy-N-phenylbenzamide derivatives, *Spectrochim. Acta A*, **188**, 213-221 (2018).
 19. Rouhani M., Khodabakhsh F., Norouzian D., Cohan R.A., Valizadeh V.; Molecular dynamics simulation for rational protein engineering: Present and future prospectus, *J. Mol. Graph. Model.*, **84**, 43-53 (2018).
 20. Becke A.D.; Density functional thermochemistry. III. The role of exact exchange; *J. Chem. Phys.*, **98**(7), 5648-5652 (1993).
 21. Lee C., Yang W., Parr R.G.; Development of the Colle-Salvetti correlation-energy formula into a functional of the electron density, *Phys. Rev. B*, **37**(2), 785(1988).
 22. Miehlich B., Savin A., Stoll H., Preuss H.; Results obtained with the correlation energy density functionals of Becke and Lee, Yang and Parr., *Chem. Phys. Lett.*, **157**(3), 200 (1989).
 23. Frisch M.J., Trucks G.W., Schlegel H.B., Scuseri G.E., Robb M.A., Cheeseman J.R., Scalmani G., Barone V., Mennucci, Petersson B. G. A., Nakatsuji H., Caricato M., Li X., Hratchian P.H., Izmaylov A.F., Bloino J., Zheng G., Sonnenberg J.L., Hada M., Ehara M., Toyota K., Fukuda R., Hasegawa J., Ishida M., Nakajima, T. Honda Y., Kitao O., Nakai H., Vreven T., Montgomery J.A., Jr., Peralta J.E., Ogliaro F., Bearpark M., Heyd J.J., Brothers, E. Kudin K.N., Staroverov V.N., Keith T., Kobayashi R., Normand, J., Raghavachari K., Rendell A., Burant J.C., Iyengar S.S., Tomasi J., Cossi M., Rega N., Millam J.M., Klene M., Knox J.E., Cross J.B., Bakken V., Adamo C., Jaramillo J., Gomperts R., Stratmann R.E., Yazyev O., Austin A.J., Cammi R., Pomelli C., Ochterski J.W., Martin R.L., Morokuma K., Zakrzewski V.G., Voth G.A., Salvador P., Dannenberg J.J., Dapprich S., Daniels A.D., Farkas, O., Foresman J.B., Ortiz J.V., Cioslowski J., Fox D.J., Gaussian, Inc., Gaussian 09, Revision C.01. Wallingford CT (2010).
 24. Ibrahim M., El-Haes H.; Computational spectroscopic study of copper, cadmium, lead and zinc interactions in the environment, *Int. J. Environ. Pollut.*, **23**, 417-424 (2005).
 25. Ibrahim M., Mahmoud A.-A.; Computational Notes on the Reactivity of some Functional Groups, *J. Comput. Theor. Nanosci.*, **6**, 1523-1526 (2009).
 26. Politzer P., Laurence P.R., Jayasuriya K.; Molecular electrostatic potentials: an effective tool for the elucidation of biochemical phenomena, *Environ. Health Persp.*, **61**, 191-202 (1985).
 27. Politzer P., Murray J.S.; Molecular Electrostatic Potentials: Concepts and Applications, *J. Theor. Comput. Chem.*, **3**, 649 (1996).
 28. Şahin Z.S., Şenöz H.I., Tezcan H., Büyükgüngör O.; Synthesis, spectral analysis, structural elucidation and quantum chemical studies of (E)-methyl-4-[(2-phenylhydrazono)methyl]benzoate, *Spectrochim. Acta A*, **143**, 91-100 (2015).

دراسة تأثير الرطوبة على الخواص الالكترونية لكاربوكسى ميثيل سليولوز الصوديوم كمركب احادي وثنائي و ثلاثي و رباعي الجزئ

رانيا بدري^{1*}، شريف الخضري²، حنان الحاييس¹، نادرة ندا¹ و مدحت ابراهيم³
¹ قسم الفيزياء، كلية النبات للأدب و العلوم و التربية، جامعة عين شمس، 11757 القاهرة، مصر.
² معهد البيئة و فيزياء المنشآت، المركز القومي لبحوث الإسكان و البناء، 12311 الدقى، الجيزة، مصر.
³ قسم الطيف، المركز القومي للبحوث، 33 شارع البحوث، 12622 الدقى، الجيزة، مصر.

وفقا للدراسات السابقة على تأثير الرطوبة التى نصت على ان الرطوبة قد تحسن الخواص الالكترونية للمواد البوليمرية. أجريت هذه الدراسة باستخدام نظرية الكثافة الوظيفية (DFT) عند مستوى (B3LYP/3-21G*) للتحقق من تأثير الرطوبة على كاربوكسى ميثيل سليولوز الصوديوم كمركب احادي وثنائي و ثلاثي و رباعي الجزئ. اشارت النتائج الى انه بسبب الرطوبة يزداد عزم ثنائى القطب الكلى بينما تقل طاقة الفجوة بين اعلى مستوى جزيئى مشغول و ادنى مستوى جزيئى غير مشغول و ذلك للمركبات الاربعة المقترحة للكاربوكسى ميثيل سليولوز الصوديوم. اشارت كل النتائج الى انه هناك تغييرات تحدث فى الخواص الالكترونية بسبب الرطوبة. و علاوة على ذلك فانه نتيجة لزيادة عدد الجزيئات يزداد عزم ثنائى القطب الكلى و يساوى (7.7141 و 28.0388 و 24.0199 و 38.3463 ديباي) للمركبات احادي وثنائي و ثلاثي و رباعي الجزئ على الترتيب. و مع ذلك قلت طاقة الفجوة بين اعلى مستوى جزيئى مشغول و ادنى مستوى جزيئى غير مشغول و تساوى (0.9040 و 0.3448 و 0.1241 و 0.9021 إلكترون فولت) على الترتيب. اضافة الى نتائج دراسة الجهد الكهربائي كانت نماذج الجزيئات فى حالة اتفاق جيد مع نتائج عزم ثنائى القطب الكلى و طاقة الفجوة بين اعلى مستوى جزيئى مشغول و ادنى مستوى جزيئى غير مشغول.